SINTEF
PROCEEDINGS
2

Proceedings of the 12th International Conference on Computational Fluid Dynamics in the Oil & Gas, Metallurgical and Process Industries

Progress in Applied CFD – CFD2017

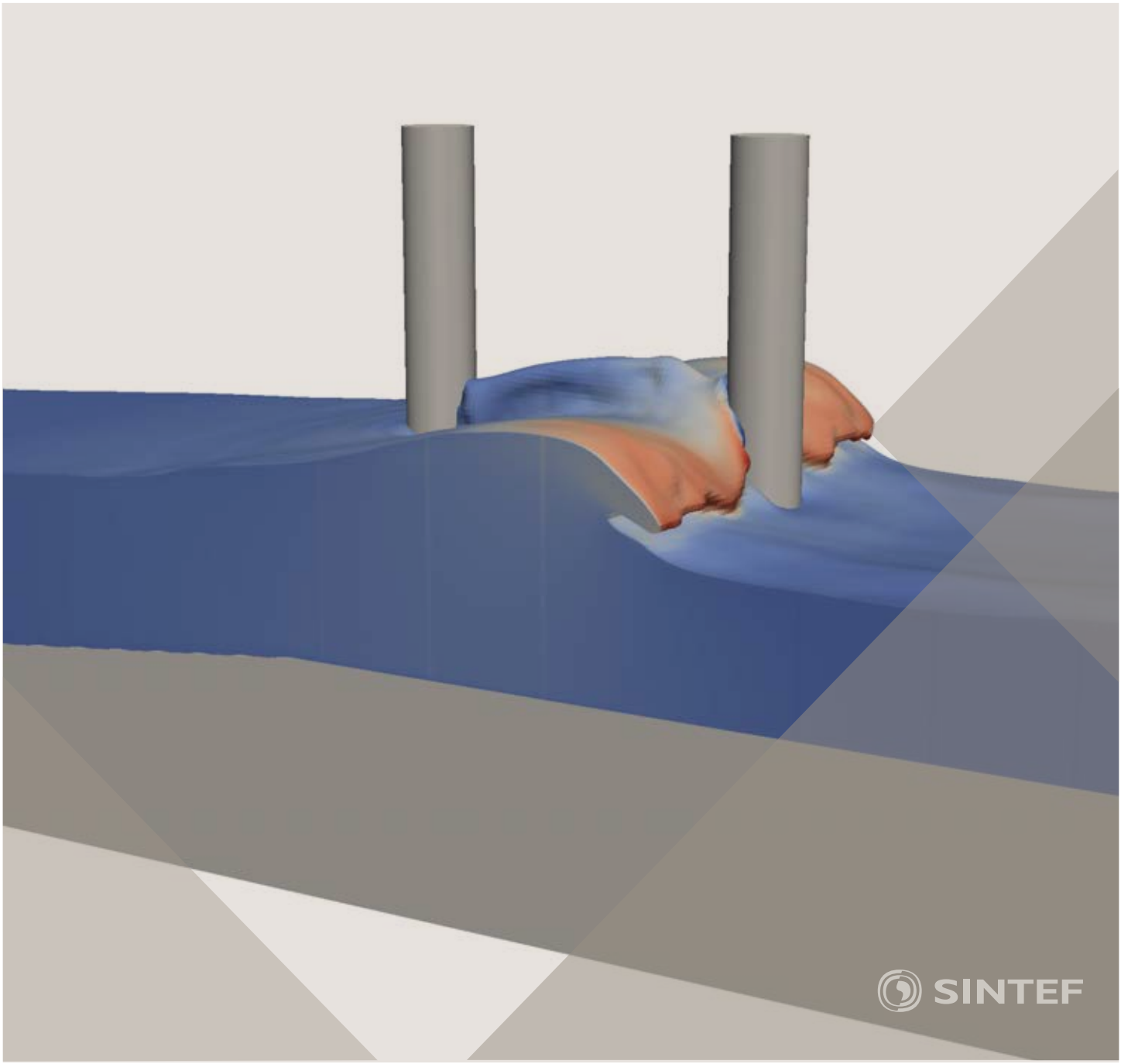

SINTEF Proceedings

Editors:
Jan Erik Olsen and Stein Tore Johansen

Progress in Applied CFD – CFD2017

Proceedings of the 12th International Conference on Computational Fluid Dynamics in the Oil & Gas, Metallurgical and Process Industries

SINTEF Academic Press

SINTEF Proceedings no 2
Editors: Jan Erik Olsen and Stein Tore Johansen
Progress in Applied CFD – CFD2017
Selected papers from 10th International Conference on Computational Fluid Dynamics in the Oil & Gas, Metallurgical and Process Industries

Key words:
CFD, Flow, Modelling

Cover, illustration: Arun Kamath

ISSN 2387-4295 (online)
ISBN 978-82-536-1544-8 (pdf)

SINTEF Academic Press
Address: Forskningsveien 3 B
PO Box 124 Blindern
N-0314 OSLO
Tel: +47 73 59 30 00
Fax: +47 22 96 55 08

www.sintef.no/byggforsk
www.sintefbok.no

SINTEF Proceedings
SINTEF Proceedings is a serial publication for peer-reviewed conference proceedings on a variety of scientific topics.
The processes of peer-reviewing of papers published in SINTEF Proceedings are administered by the conference organizers and proceedings editors. Detailed procedures will vary according to custom and practice in each scientific community.

PREFACE

This book contains all manuscripts approved by the reviewers and the organizing committee of the 12th International Conference on Computational Fluid Dynamics in the Oil & Gas, Metallurgical and Process Industries. The conference was hosted by SINTEF in Trondheim in May/June 2017 and is also known as CFD2017 for short. The conference series was initiated by CSIRO and Phil Schwarz in 1997. So far the conference has been alternating between CSIRO in Melbourne and SINTEF in Trondheim. The conferences focuses on the application of CFD in the oil and gas industries, metal production, mineral processing, power generation, chemicals and other process industries. In addition pragmatic modelling concepts and bio-mechanical applications have become an important part of the conference. The papers in this book demonstrate the current progress in applied CFD.

The conference papers undergo a review process involving two experts. Only papers accepted by the reviewers are included in the proceedings. 108 contributions were presented at the conference together with six keynote presentations. A majority of these contributions are presented by their manuscript in this collection (a few were granted to present without an accompanying manuscript).

The organizing committee would like to thank everyone who has helped with review of manuscripts, all those who helped to promote the conference and all authors who have submitted scientific contributions. We are also grateful for the support from the conference sponsors: ANSYS, SFI Metal Production and NanoSim.

Stein Tore Johansen & Jan Erik Olsen

Organizing committee:

Conference chairman: Prof. Stein Tore Johansen
Conference coordinator: Dr. Jan Erik Olsen
Dr. Bernhard Müller
Dr.Sigrid Karstad Dahl
Dr.Shahriar Amini
Dr.Ernst Meese
Dr.Josip Zoric
Dr.Jannike Solsvik
Dr.Peter Witt

Scientific committee:

Stein Tore Johansen, SINTEF/NTNU
Bernhard Müller, NTNU
Phil Schwarz, CSIRO
Akio Tomiyama, Kobe University
Hans Kuipers, Eindhoven University of Technology
Jinghai Li, Chinese Academy of Science
Markus Braun, Ansys
Simon Lo, CD-adapco
Patrick Segers, Universiteit Gent
Jiyuan Tu, RMIT
Jos Derksen, University of Aberdeen
Dmitry Eskin, Schlumberger-Doll Research
Pär Jönsson, KTH
Stefan Pirker, Johannes Kepler University
Josip Zoric, SINTEF

CONTENTS

12th International Conference on CFD in Oil & Gas, Metallurgical and Process Industries
SINTEF, Trondheim, NORWAY
May 30th - June 1st, 2017

LES-VOF SIMULATION OF TURBULENT INTERFACIAL FLOW IN THE CONTINUOUS CASTING MOLD

Mahdi SAEEDIPOUR[1,2*], **Stefan PUTTINGER**[1†], **Stefan PIRKER**[1‡]

[1]Department of Particulate Flow Modelling, Johannes Kepler University, 4040 Linz, AUSTRIA

[2]Christian Doppler Laboratory for Multi-scale Modeling of Multiphase Processes, Johannes Kepler University, 4040 Linz, AUSTRIA

* E-mail: mahdi.saeedipour@jku.at
† E-mail: stefan.puttinger@jku.at
‡ E-mail: stefan.pirker@jku.at

ABSTRACT

Slag entrainment during continuous casting process is a multiscale problem strongly dependent on the molten metal flow in the mold. Large-scale flow structures in the mold interact with the slag layer at the top of the meniscus, and small-scale liquid structures in the form of slag droplets may be entrained into the solidifying metal. In this work a large eddy simulation - volume of fluid (LES-VOF) approach is applied to investigate the unsteady flow interaction with the metal-slag-air interface including the interface instability, deformation of the slag layer and its entrainment into the molten metal.

A benchmark experiment was designed to investigate the flow field in the proximity of a liquid-liquid interface for validation purposes. The experiment uses water and paraffinum liquidum to model the combination of liquid steel and the slag layer. While the entrainment of oil droplets can be visualized via shadowgraphy the flow field was measured via particle image velocimetry PIV. In combination, these two methods allow a qualitative and quantitative comparison of the unsteady flow characteristics with the CFD results.

The measurement data at different inflow conditions have been used to validate the simulation results. We compare the global flow characteristics and mean velocity of submerged entry nozzle jet upon injection to the mold. Furthermore, the statistics of turbulence including velocity fluctuations and turbulent kinetic energy are used to investigate the unsteady jet interaction with the slag layer as well as liquid-liquid interface dynamics. The comparison of CFD results and experimental data reveals fairly good agreement both quantitatively and qualitatively.

Keywords: Two-phase interfacial flow, large eddy simulation (LES), volume of fluid (VOF), particle image velocimetry (PIV), slag entrainment, continuous casting .

NOMENCLATURE

Greek Symbols

ρ	Mass density, $[kg/m^3]$
μ	Dynamic viscosity, $[kg/ms]$
σ	Surface tension coefficient, $[N/m]$
α	Volume of fluid, $[-]$
μ	Dynamic viscosity, $[kg/ms]$
δ	Kronecker delta tensor, $[-]$
ϕ	Arbitrary flow quantity, $[-]$
τ	Sub-grid term, $[-]$
Δ	Grid size, $[m]$
κ	Curvature, $[1/m]$
$\mathcal{G}$	Spatial filter operator, $[-]$
Θ	Inlet angle, $[deg]$

Latin Symbols

p	Pressure, $[Pa]$.
$\mathbf{U}$	Velocity, $[m/s]$.
$\mathbf{S}_\sigma$	Surface tension force, $[N]$.
$\mathbf{D}$	Rate of deformation, $[1/s]$.
$\mathbf{n}$	Interface normal vector, $[-]$.
C_s	Smagorinsky constant, $[-]$.

Sub/superscripts

a	air.
o	oil.
w	water.
i	Index i.
j	Index j.

INTRODUCTION

Many industrial and environmental processes involve highly unsteady turbulent interfacial flows. Examples include liquid jet breakup, petroleum transportation, continuous casting process and many others. In continuous casting molds, the top surface of molten steel is covered by a slag layer in order to prevent steel from oxidation and heat loss as well as to use it as a lubricant between the solidifying steel and the mold (Iguchi *et al.*, 2000). Slag entrainment affects the quality of the final product strongly, if the entrained droplets become trapped in the solidifying metal. This draws much attention to the fundamental studying of slag entrainment in the casting industry over the recent decades, resulting in several proposed mechanisms (Hibbeler and Thomas, 2013).

According to several experimental investigations on mold flow, the shear-layer instability between the slag and molten metal, known as Kelvin-Helmholtz instability, has been identified as one of the mechanisms of slag entrainment. In addition, the formation of vortices behind the submerged entry nozzle (SEN), known as Karman vortex, can cause slag entrainment by pulling the slag layer down into the molten metal. It is also discussed by Iguchi *et al.* (2000) that the argon gas injection into the SEN to prevent clogging will result in bubble formation in the mold. The interaction between these bubbles and the slag interface is also introduced as another mechanism of slag entrainment.

All mentioned mechanisms are associated with the unsteady flow situation near the interface in particular due to the turbulence of the liquid steel pool (see Figure 1). Numerical simulation of such a multiphase turbulent flow remains a chal-

lenging topic, because a prospective approach must account for the turbulence modelling as well as capturing the interfacial topology between phases.

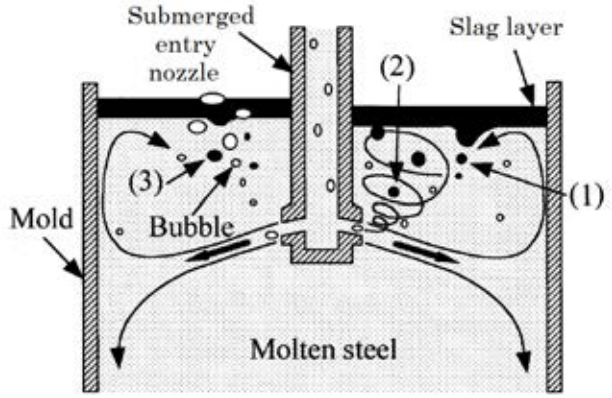

Figure 1: Schematic of slag entrainment mechanisms (reproduced from Iguchi *et al.* (2000)).

A variety of numerical studies on turbulent multiphase flows with different industrial application have been done within the last decade. In the case of modelling the continuous casting mold flow, Liu *et al.* (2013) carried out large eddy simulations to study the effect of argon gas injection through the SEN on the flow pattern in the mold. In this study they employed an Euler-Euler approach to model the molten metal flow and argon bubbles. In a similar work, they coupled a Lagrangian model with two-fluid model to study the influence of argon gas injection on the molten steel flow and particle transport behaviors (Liu *et al.*, 2014). Vakhrushev *et al.* (2014) studied the global behavior of mold flow around the SEN using a volume of fluid method. In this work a RANS-based turbulence model (i.e. $k-\varepsilon$) was coupled to three-phase VOF model to obtain the velocity field and the time-averaged oil-water interface position. They also validated the numerical results with a 1/3 scaled-down water model. Recently, the transient free surface behavior in a model mold is studied by Asad *et al.* (2015) using a RANS-VOF approach. In this work the impact of inlet velocity and nozzle depth on the free surface behavior and flow pattern was investigated and different flow regimes in the mold were observed.

Most of the aforementioned studies employed the RANS-based turbulence models which can only capture the global behavior of the unsteady flow in a large-scale domain; however, there are many small-scale phenomena involved in the slag entrainment that need to be captured by the numerical tool. Although RANS methods are computationally-efficient for industrial flow, they are not capable of capturing small-scale physics of multiphase flows. Even those studies that carried out LES do not report the conditions where several droplet-like slag structures are generated from the interface. Nevertheless, the entrainment of slag droplets into the water pool is observed in present benchmark experiments.

In the present work we aim at studying the mold flow three-phase using an LES-VOF approach which then provides us with an in-depth understanding of the physics of the flow in both large and small scales. Furthermore, the water-oil benchmark experiment is designed to visualize the global mold flow and measure the unsteady flow using PIV. The simulation results are then validated against the experiments at different conditions. The combination of experiments and modelling helps us to realize the shortcomings of LES approach in modelling of slag entrainment, especially at critical conditions result in dispersed multiphase flow.

MODEL DESCRIPTION

Governing equations

From computational point of view, a feasible modelling strategy for interfacial turbulent flows including metal-slag-air flow in the continuous casting mold, must include proper treatment for (i) fluid flow governing equations (i.e. Navier-Stokes equations), (ii) capturing the interface between phases (i.e. VOF method (Hirt and Nichols, 1981) in the present study) and (iii) turbulence modelling. Therefore, the conservation equations governing the fully resolved motion of an unsteady, incompressible, immiscible, multiphase flow with single-fluid formulation are the continuity and Navier-Stokes equations together with the transport equation of volume of fluid as follows:

$$\frac{\partial \rho}{\partial t} + \nabla \cdot (\rho \mathbf{U}) = 0 \tag{1}$$

$$\frac{\partial (\rho \mathbf{U})}{\partial t} + \nabla \cdot (\rho \mathbf{U} \otimes \mathbf{U}) = -\nabla p + \nabla \cdot (2\mu \mathbf{D}) + \rho \mathbf{g} + \mathbf{S}_\sigma \tag{2}$$

$$\frac{\partial \alpha}{\partial t} + \nabla \cdot (\alpha \mathbf{U}) = 0 \tag{3}$$

For incompressible flows where $\rho = const$, the continuity equation reduces to $\nabla \cdot \mathbf{U} = 0$.

In this single-fluid formulation, $\vec{\mathbf{U}}$ is the mixture velocity field shared with all phases. p is the pressure and $\mathbf{D}$ is the rate of deformation tensor in the form of $\mathbf{D} = \frac{1}{2}(\nabla \mathbf{U} + \nabla^T \mathbf{U})$. The scalar function α is the volume of fluid field which determines the physical properties of the flow in one-fluid formulation based on properties of each phase, as follows:

$$\rho = \alpha \rho_1 + (1-\alpha)\rho_2 \tag{4a}$$

$$\mu = \alpha \mu_1 + (1-\alpha)\mu_2 \tag{4b}$$

$\mathbf{S}_\sigma$ is the surface tension force which is treated by the Continuous Surface Force (CSF) method (Brackbill *et al.*, 1992). This method considers surface tension effects as a volumetric source term in the momentum equation acting only on the interfacial areas. Following the CSF method, the interface normal vector $\hat{\mathbf{n}}$ and interface curvature κ (i.e. the first and second derivatives of the phase indicator function) are of significant importance in the determination of the surface tension force.

The most common method in estimation of the curvature and normal vector for each computational cell is based on interface orientation approach by Youngs (1982). In this approach a basic definition of interface normal vector is applied based on the gradient of VOF function, then the unit interface normal, and its curvature are determined as

$$\hat{\mathbf{n}} = \frac{\nabla \alpha}{|\nabla \alpha|} \tag{5}$$

$$\kappa = -\nabla \cdot \hat{\mathbf{n}} = -\nabla \cdot \left(\frac{\nabla \alpha}{|\nabla \alpha|} \right) \tag{6}$$

Finally, the surface tension force can be computed by the CSF method and reads

$$\mathbf{S}_\sigma = \sigma\kappa\hat{\mathbf{n}}\delta_s \tag{7}$$

where σ is the surface tension coefficient and δ_s is the Dirac delta function that equals unity at the interface and zero elsewhere. The numerical procedure to solve this system of equations for two phases is implemented in the open source CFD framework of OpenFOAM (Greenshields, 2015) within the solver called *interFoam*. As an extension to this solver, for the multiphase flows with more than two different phases, the solver *multiphaseInterFoam* is adopted. The main difference between these two solvers is the way for computation of the curvature. *multiphaseInterFoam* uses a pair-averaged gradient of the volume fraction (Vakhrushev *et al.*, 2014) for computing the unit interface normal in equation (5). Thus $\hat{\mathbf{n}}$ is reformulated for interface between each pair of phases and reads

$$\hat{\mathbf{n}}_{ij} = \frac{\alpha_j\nabla\alpha_i - \alpha_i\nabla\alpha_j}{\mid \alpha_j\nabla\alpha_i - \alpha_i\nabla\alpha_j \mid} \tag{8}$$

where α_i and α_j are the volume fractions of each pair of phases (i, j). This solver is utilized in the present study to capture the interface between molten metal, slag and air. It should be noted that the equations (4a) and (4b) are also including the third phase properties to be consistent with the mixture assumption.

Large eddy simulation

Large eddy simulation (LES) is typically considered as an intermediate approach for modelling turbulent flows. The principal idea behind LES is to reduce the computational efforts by spatial filtering the small-scale motions (i.e. by a low-pass filter operation) and only resolve the largest ones. By applying a spatial filter operator $\mathcal{G}$ to a flow quantity $\phi(\mathbf{x},t)$, the filtered quantity reads:

$$\overline{\phi}(\mathbf{x},t) = \mathcal{G} * \phi(\mathbf{x},t) = \int_D \mathcal{G}(\mathbf{x}-\mathbf{x}')\phi(\mathbf{x}',t)\,\mathrm{d}\mathbf{x}' \tag{9}$$

where $(\bar{\cdot})$ indicates the spatial filtering.

Introducing the filter operation into equations (1) to (3) and assuming that the filter commutes with both the time and spatial derivatives, the filtered governing equations can be derived as follows:

$$\nabla\cdot\overline{\mathbf{U}} = 0 \tag{10a}$$

$$\frac{\partial(\overline{\rho}\overline{\mathbf{U}})}{\partial t} + \nabla\cdot(\overline{\rho}\overline{\mathbf{U}}\otimes\overline{\mathbf{U}}) = -\nabla\overline{p} + \nabla\cdot(2\overline{\mu}\overline{D}) + \rho\vec{\mathbf{g}} + \sigma\overline{\kappa}\nabla\overline{\alpha} + \nabla\cdot(\tau_{\mu D} - \tau_{uu}) + \tau_\sigma - \tau_{tt} \tag{10b}$$

$$\frac{\partial\overline{\alpha}}{\partial t} + \nabla\cdot(\overline{\alpha}\overline{\mathbf{U}}) = \nabla\cdot\tau_{\alpha u} \tag{10c}$$

This operation results in appearance of different sub-grid scale (SGS) terms in the equations.

$$\tau_{uu} = \overline{\rho\mathbf{U}\otimes\mathbf{U}} - \overline{\rho}\overline{\mathbf{U}}\otimes\overline{\mathbf{U}} \tag{11a}$$

$$\tau_{\mu D} = \overline{\mu(\nabla\mathbf{U} + \nabla^T\mathbf{U})} - \overline{\mu}(\nabla\overline{\mathbf{U}} + \nabla^T\overline{\mathbf{U}}) \tag{11b}$$

$$\tau_{tt} = \frac{\partial(\overline{\rho\mathbf{U}})}{\partial t} - \frac{\partial(\overline{\rho}\overline{\mathbf{U}})}{\partial t} \tag{11c}$$

$$\tau_\sigma = \sigma\overline{\kappa\nabla\alpha} - \sigma\overline{\kappa}\nabla\overline{\alpha} \tag{11d}$$

$$\tau_{\alpha u} = \overline{\alpha}\overline{\mathbf{U}} - \overline{\alpha\mathbf{U}} \tag{11e}$$

The sub-grid scale of convective, viscous and unsteady terms in equations (11a) to (11c) are present in classical single phase LES while the sub-grid surface tension effects as well as the sub-grid of interfacial transport in equations (11d) and (11e) appear specifically in two-phase flows.
It is reported by several DNS studies that in most of single phase turbulent flows, the contribution of the sub-grid scale convective term to the turbulent kinetic energy budget is predominant (Labourasse *et al.*, 2007). This provides the basis for the closure of the single phase LES formulation by the eddy-viscosity approach (Versteeg and Malalasekera, 2006). Nevertheless, in the context of turbulent interfacial flows, the contribution of sub-grid scale surface tension and volume of fluid transport is not negligible specially at small-scale interfacial topological changes. But due to the lack of general model for those sub-grid terms, only the sub-grid convective term is accounted for in the present study. Therefore, the anisotropic part of the sub-grid stress tensor is modelled by eddy-viscosity approximation as follows:

$$\tau_{uu} - \frac{1}{3}\mathrm{Tr}(\tau_{uu})\mathbf{I} = -2\mu_t\overline{\mathbf{D}} \tag{12}$$

In this formulation, the turbulent eddy-viscosity reads

$$\mu_t = (C_s\Delta)^2 \mid \overline{\mathbf{D}} \mid \tag{13}$$

where C_s is the model constant and Δ is the grid size. As the turbulence modelling is a generic feature of most of the OpenFOAM solvers, the classical Smagorinsky model (Smagorinsky, 1963) is chosen in *multiphaseInterFoam* to close the system of equations.

EXPERIMENTS

To provide experimental data for comparison with our CFD model we built up a simplified mold flow experiment in the lab as shown in Figure 2. It represents a 1/3 model of a continuous casting mold. As a replacement for steel and slag we use water and colored paraffinum oil. In order to investigate the interaction of the jet with the water-oil interface for various inlet angles (Θ), we use a central symmetry plane with an adjustable inlet nozzle instead of a SEN. This gives more flexibility and allows to check worst case scenarios with strong interaction of the jet with the liquid-liquid interface for positive inlet angles. The water circuit is driven by an impeller pump and all shown results were obtained at a flow rate of 0.26 l/s. To avoid upstream disturbances in the mold flow caused by the water outlet, the main basin is decoupled from the outlet area by a porous plate. The dimensions of the experiment are shown in Table 1. The physical properties of water and paraffinum oil are found in Table 2.
Data is recorded with an ordinary video camera to get a qualitative impression of the jet-interface interaction and slag entrainment as well as 2D particle image velocimetry (PIV). In the latter case the center plane of the basin is illuminated with

Table 1: Dimensions of the lab experiment.

Dimensions	250 x 400 x 75 mm
Diameter of inlet nozzle	19 mm
Water level above inlet	8 cm
Thickness of oil layer	1.5 cm

Table 2: Physical properties of water and paraffinum oil at $20^{\circ}C$.

Water (w)			Paraffinum Liquidum (o)		
μ	1	mPa · s	μ	189	mPa · s
ρ	1000	kg/m^3	ρ	863.3	kg/m^3
σ	0.07275	N/m	σ	0.026	N/m

a Nd:YAG laser and plastic powder is used as tracer particles for PIV processing. A total number of 1000 double frames is recorded for each case to provide sufficient data for averaging the flow fields.
For comparison of CFD results with experimental data both data sources are interpolated to a common equidistant grid using MATLAB.

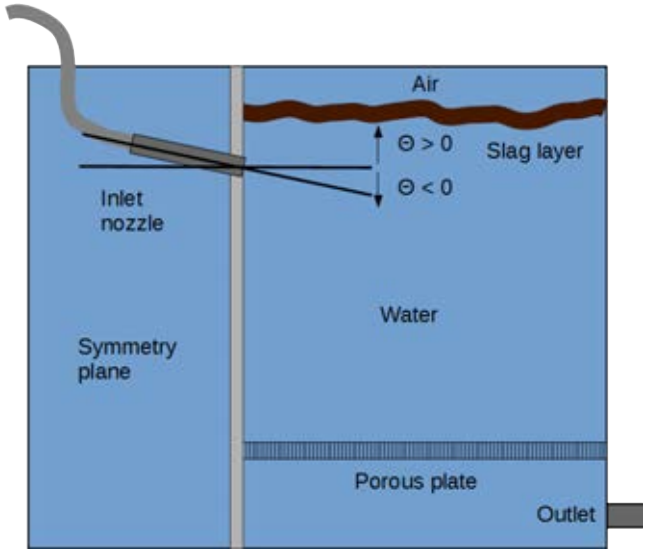

Figure 2: The sketch of lab experiment.

RESULTS AND DISCUSSION

Simulation setup

In order to perform numerical simulation, a three-dimensional geometry ($L_x = 250$ mm, $L_y = 400$ mm and $L_z = 70$ mm) with a circular inlet was created as the computational domain. Then structured computational grid networks were generated with the lowest grid spacing of 1.5 *mm* as shown in Figure 3. The initial value of volume fraction for each phase is adjusted similar to the experimental case.
Pressure outlet and wall boundary conditions were imposed on the surrounding boundaries of computational domain. Since generating inflow boundary conditions for LES is not a straightforward task, a turbulent velocity boundary condition was used at the inlet to initiate the injection with a randomly-perturbed velocity profile with the intensity of 0.1. The PIMPLE algorithm is adopted for pressure-velocity coupling and pressure correction. The VOF transport equation is solved by a specific algorithm in OpenFOAM called MULES solver (Multidimensional Universal Limiter with Explicit Solution). This method guarantees the robustness of the VOF method when using an artificial compression term to improve the interface resolution (Greenshields, 2015). The simulation time steps are determined based on CFL criterion to keep the maximum Courant number about 0.6.
All the fluid properties in the simulation were taken similar to the experiments. The interfacial tension between water and oil is $\sigma_{w/o}$= 0.048 N/m. The air properties were used at standard room temperature ρ_a= 1.2 kg/m^3 and μ_a= 0.017 mPa·s.

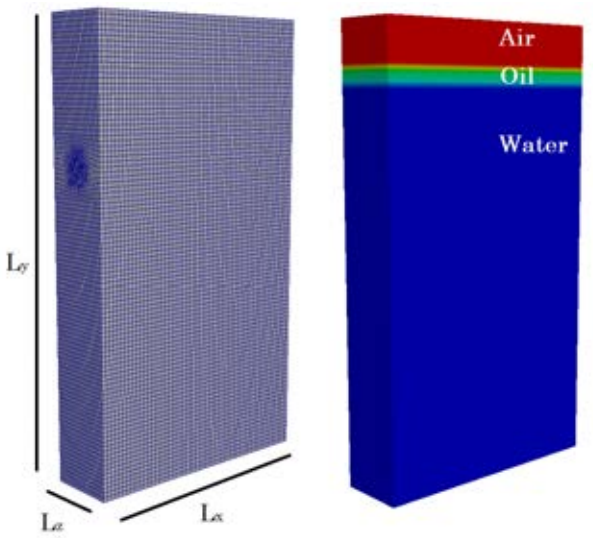

Figure 3: The sketch of computational domain.

Global flow characteristics

Numerical simulations were performed for two cases at different inlet angles of Θ = -10 and 0 degree. In order to validate the CFD results with PIV measurements, the first quantity to look at is the average velocity field in the mold. For this purpose the simulations were run long enough to obtain sufficient instantaneous velocity fields at every 5 ms at the mid-plane in z-direction. The average velocity magnitude from the CFD results for Θ = -10 and 0 degree are shown in Figures 4 and 5, respectively. To reveal a comparison with the PIV results, the average velocity profiles from CFD and experiments are plotted along with the constant horizontal and vertical distances of $x = 200$ mm and $y = 70$ mm as shown in Figures 6 to 9. The overall comparison demonstrates fairly good agreement between the simulation and experiments.
Furthermore, the velocity fields obtained from the CFD simulation are used to compute the energy spectra. Therefore, a fast Fourier transform was carried out and the energy spectrum reveals that the present LES model yields good agreement with the Kolmogorov spectrum (Pope, 2000). However, for validating the dynamic behavior of the CFD simulation we need time-resolved experimental data, which we will obtain by high-speed PIV in the near future.

Slag entrainment depth

To investigate the interaction of the mold flow with the slag layer we extracted the point of maximum slag entrainment depth. Figure10 shows an example of the shadowgraphy experiments where the colored layer of oil can be clearly distinguished from the water phase. The position of the deepest oil entrainment can simply be extracted via digital image processing. The same procedure was applied to CFD data

by using the volume of fluid field of oil at iso-surfaces of $\alpha_o = 0.5$. The CFD and experimental results are compared in Figures 11 and 12 for the cases with $\Theta = -10$ and 0 degree inclination, respectively. One can see that the positions of maximum slag entrainment correspond quite well between CFD and experimental results. Nevertheless the spreading of data in the experiment is larger which can also be noticed as a higher dynamics of the interface movement in the recorded videos.

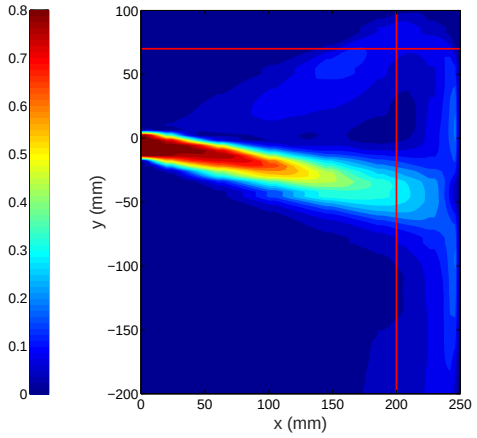

Figure 4: The average velocity magnitude at mid-plane for $\Theta = -10$ deg. The contour is plotted in SI unit.

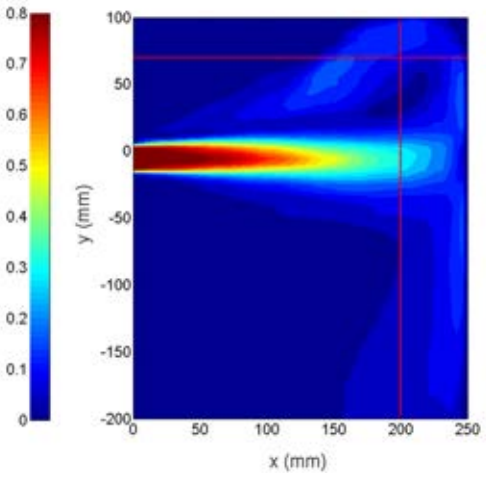

Figure 5: The average velocity magnitude at mid-plane for $\Theta = 0$ deg. The contour is plotted in SI unit.

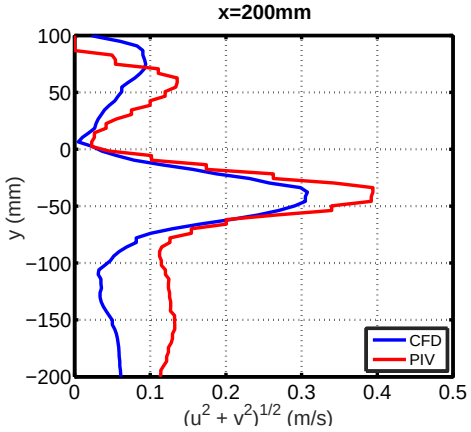

Figure 6: CFD-PIV comparison of the average velocity profile at $x = 200$ mm for $\Theta = -10$ deg.

CONCLUSION AND OUTLOOK

In this paper, the turbulent interfacial flow in the continuous casting mold was numerically and experimentally studied. An LES-VOF approach is applied to investigate the unsteady flow interaction with the metal-slag-air interface. A water-oil benchmark experiment was designed for validation purposes. While the entrainment of slag into the mold was

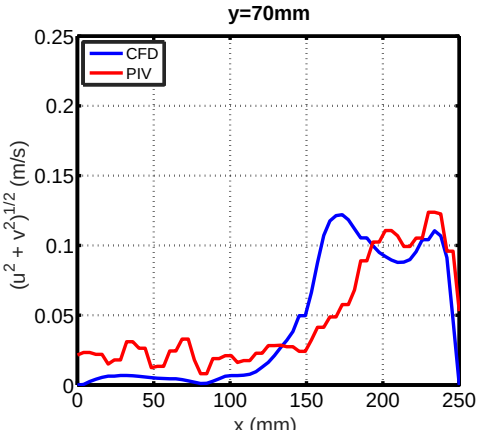

Figure 7: CFD-PIV comparison of the average velocity profile at $y = 70$ mm for $\Theta = -10$ deg.

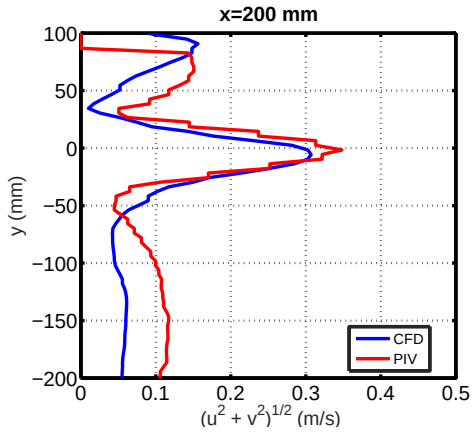

Figure 8: CFD-PIV comparison of the average velocity profile at $x = 200$ mm for $\Theta = 0$ deg.

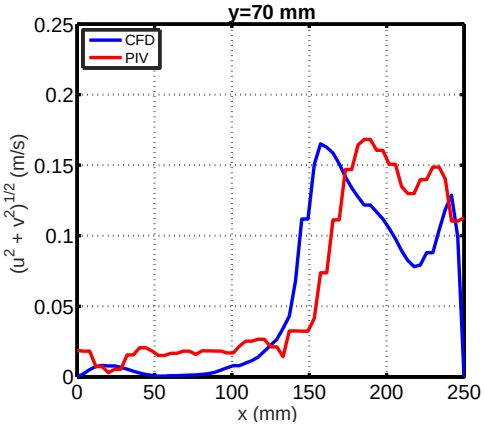

Figure 9: CFD-PIV comparison of the average velocity profile at $y = 70$ mm for $\Theta = 0$ deg.

visualized via shadowgraphy, the flow field was measured via particle image velocimetry. In combination these two methods allow a qualitative and quantitative comparison of the unsteady flow characteristics with the CFD results. First, we compared the global flow behavior for different inflow conditions by using the average velocity fields obtained from the CFD and PIV. The general agreement of CFD results and experimental data is very promising. Then, we investigated the interaction of the unsteady flow field with the liquid-liquid interface. The entrainment depth from the simulation match the experimental visualization quite well while the dynamics of the interface motion is much lower in the CFD simulation than in the experiments.

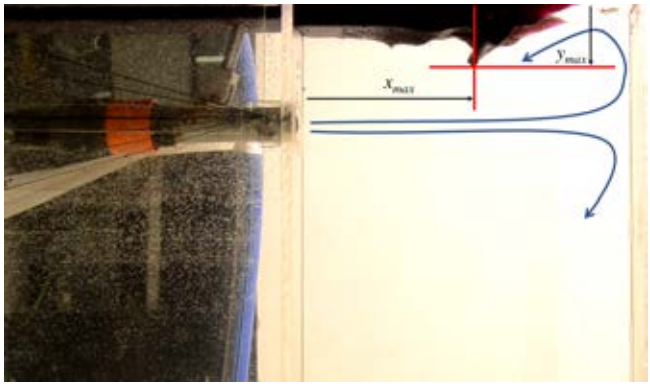

Figure 10: Example image from the mold flow experiment showing the position of maximum slag layer entrainment.

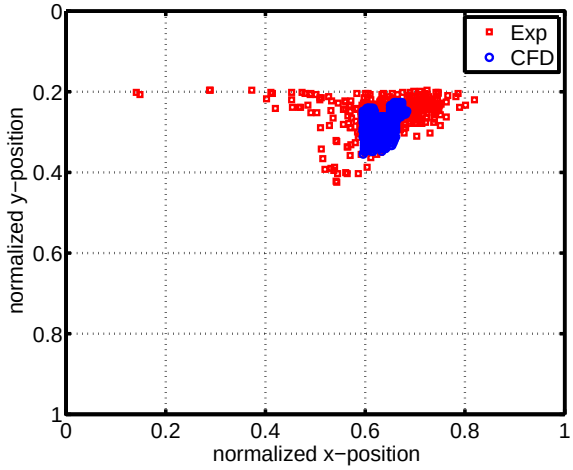

Figure 11: The positions of maximum slag entrainment for $\Theta = -10$ degree from simulation and experiment.

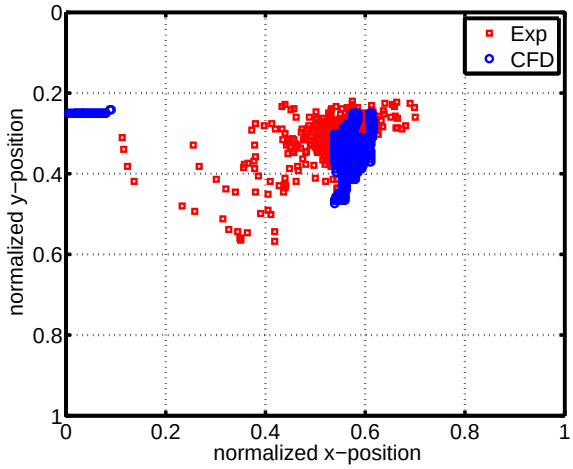

Figure 12: The positions of maximum slag entrainment for $\Theta = 0$ degree from simulation and experiment.

However, there are some shortcomings to be considered for future improvements of the model such as employing a more accurate inflow boundary condition for LES simulation. Although the entrainment of small-scale oil droplets cannot be captured with the current level of modelling, it can be deduced that LES-VOF approach is a feasible way to model the slag entrainment at critical conditions where the droplet-like slag structures become dispersed in the mold. To this end, improvement of the current LES-VOF by sub-grid modification seems inevitable. Future studies will also focus on numerical modelling and experimental investigation of other mechanisms for slag entrainment including the Karman vortex formation.

ACKNOWLEDGMENTS

The authors gratefully acknowledge the funding support of K1-MET GmbH, metallurgical competence center. The research program of the competence center K1-MET is supported by COMET (Competence Center for Excellent Technologies), the Austrian program for competence centers. COMET is funded by the Federal Ministry for Transport, Innovation and Technology, the Federal Ministry for Science, Research and Economy, the province of Upper Austria, Tyrol, and Styria and the Styrian Business Promotion Agency.

REFERENCES

ASAD, A., KRATZSCH, C. and SCHWARZE, R. (2015). "Numerical Investigation of the Free Surface in a Model Mold". *Steel Research International*, **86**, 1–10.

BRACKBILL, J., KOTHE, D. and ZEMACH, C. (1992). "A continuum method for modeling surface tension". *Journal of Computational Physics*, **100**, 335–354.

GREENSHIELDS, C.J. (2015). "OpenFOAM The Open Source CFD Toolbox". Tech. rep. URL `http://www.openfoam.com`.

HIBBELER, L.C. and THOMAS, B.G. (2013). "Mold slag entrainment mechanisms in continuous casting molds". *Iron and Steel Technology*, **10(10)**, 121–136.

HIRT, C. and NICHOLS, B. (1981). "Volume of fluid (VOF) method for the dynamics of free boundaries". *Journal of Computational Physics*, **39**, 201–225.

IGUCHI, M., YOSHIDA, J., SHIMIZU, T. and MIZUNO, Y. (2000). "Model Study on the Entrapment of Mold Powder into Molten Steel." *ISIJ International*, **40(7)**, 685–691.

LABOURASSE, E., LACANETTE, D., TOUTANT, A., LUBIN, P., VINCENT, S., LEBAIGUE, O., CALTAGIRONE, J.P. and SAGAUT, P. (2007). "Towards large eddy simulation of isothermal two-phase flows: Governing equations and a priori tests". *International Journal of Multiphase Flow*, **33(1)**, 1–39.

LIU, Z.Q., LI, B.K., JIANG, M.F. and TSUKIHASHI, F. (2013). "Modeling of Transient Two-Phase Flow in a Continuous Casting Mold Using Euler-Euler Large Eddy Simulation Scheme". *ISIJ International*, **53(3)**, 484–492.

LIU, Z.Q., LI, B.K., JIANG, M.F. and TSUKIHASHI, F. (2014). "Euler-Euler-Lagrangian Modeling for Two-Phase Flow and Particle Transport in Continuous Casting Mold". *ISIJ International*, **54(6)**, 1314–1323.

POPE, S. (2000). *Turbulent Flows*. Cambridge University Press.

SMAGORINSKY, J. (1963). "General circulation experiments with the primitive equations, I. the basic experiment". *Monthly Weather Review*, **91**, 99–164.

VAKHRUSHEV, A., WU, M., LUDWIG, A., NITZL, G., TANG, Y. and HACKL, G. (2014). "Experimental verification of a 3-phase Continuous casting simulation using a water model". *8th European Continuous Casting Conference*. Graz, Austria.

VERSTEEG, H.K. and MALALASEKERA, W. (2006). *An Introduction to Computational Fluid Dynamics Second Edition*. Pearson Education Limited.

YOUNGS, D. (1982). "Time-Dependent Multi- material Flow with Large Fluid Distortion". *Numerical methods for fluid dynamics*, 273–285. Academic Press, New York.